AD-A250 000

TECHNICAL REPORT BRL-TR-3330

BRL

INTERIOR BALLISTIC SIMULATIONS OF 25-MM GUN CHARGES

LANG-MANN CHANG

APRIL 1992

U.S. ARMY LABORATORY COMMAND

BALLISTIC RESEARCH LABORATORY
ABERDEEN PROVING GROUND, MARYLAND

NOTICES

REPORT DOCUMENTATION PAGE

Form Approved
OMB No. 0704-0188

1. AGENCY USE ONLY *(Leave blank)*	2. REPORT DATE	3. REPORT TYPE AND DATES COVERED
	April 1992	Final, June 1988 - February 1989

4. TITLE AND SUBTITLE
Interior Ballistic Simulations of 25-mm Gun Charges

5. FUNDING NUMBERS
PR: 1L162618AH80

6. AUTHOR(S)
Lang-Mann Chang

7. PERFORMING ORGANIZATION NAME(S) AND ADDRESS(ES)

8. PERFORMING ORGANIZATION REPORT NUMBER
BRL-TR-3330

9. SPONSORING MONITORING AGENCY NAME(S) AND ADDRESS(ES)
U.S. Army Ballistic Research Laboratory
ATTN: SLCBR-DD-T
Aberdeen Proving Ground, MD 21005-5066

10. SPONSORING/MONITORING AGENCY REPORT NUMBER

11. SUPPLEMENTARY NOTES

12a. DISTRIBUTION / AVAILABILITY STATEMENT
Approved for public release; distribution is unlimited.

12b. DISTRIBUTION CODE

13. ABSTRACT *(Maximum 200 words)*

Interior ballistic simulations are performed for propelling charges based on two candidate propellants for the 25-mm cannon system mounted on the Bradley Fighting Vehicle. The two propellants are a single-base propellant and a high energy LOVA propellant (HELP1). The hydrodynamics code employed in the simulations is the two-phase flow XKTC code (the latest version of the NOVA code). Two areas are emphasized in this study. One is the ballistic performance comparison for each propellant using primers in three different configurations. The other is the direct comparison of ballistic characteristics between the two propellants. Results correlate well with the experimental data obtained in previous studies. It is concluded that a primer which provides more rapid flamespreading and uniform ignition along the length of the charge results in better ballistic performance. The ignition and ballistic performance of the HELP1 propelling charge, in comparison with the single-base, are found to be more sensitive to the variation of primer configuration.

14. SUBJECT TERMS
interior ballistics, ballistic simulation, primers, LOVA propellant, 25-mm gun

15. NUMBER OF PAGES
51

16. PRICE CODE

17. SECURITY CLASSIFICATION OF REPORT	18. SECURITY CLASSIFICATION OF THIS PAGE	19. SECURITY CLASSIFICATION OF ABSTRACT	20. LIMITATION OF ABSTRACT
UNCLASSIFIED	UNCLASSIFIED	UNCLASSIFIED	UL

INTENTIONALLY LEFT BLANK.

TABLE OF CONTENTS

INTENTIONALLY LEFT BLANK.

LIST OF FIGURES

INTENTIONALLY LEFT BLANK.

LIST OF TABLES

INTENTIONALLY LEFT BLANK.

ACKNOWLEDGMENTS

The author wishes to thank Messrs. F. Robbins and K. Resnik for their assistance in setting up the job streams to run the XKTC code and graphics routines. Thanks are also due to Mr. M. Bonnano of NOSIH in furnishing the physical and chemical properties of the HELP1 propellant used in this study.

INTENTIONALLY LEFT BLANK.

1. INTRODUCTION

High performance LOVA propelling charges have been proposed to replace the conventional propelling charges in use for the 25-mm cannon system mounted on the Bradley Fighting Vehicle to reduce the vulnerability of the vehicle. As part of the effort in developing the low-vulnerability ammunition, charge ignition studies and interior ballistic simulations have been conducted. The ignition studies have been carried out via a gun simulator and the ballistic simulations have been performed utilizing the XNOVAKTC (XKTC) code (Gough 1990). While the simulator diagnostics provide insights into the phenomena occurring in the ignition phase, the computer simulations can evaluate the ballistic performance. These two efforts are to establish a guideline for selection of an effective ignition system and a LOVA propelling charge for the cannon system. The present report focuses on the computer simulation work, while the experimental simulator diagnostics study has been reported in Chang and Bonanno (1987).

In the simulator diagnostics, the ignition phenomena resulting from the use of three different primer configurations (designated MK0, MK1, and MK2) were investigated. Figure 1 depicts these primers when inserted into the cartridge case base. The MK0 primer was simply the standard M115 primer used in the conventional 25-mm cannon ammunition. The MK1 and MK2 primers were constructed by adding a tube 24.5 mm in length and a tube 50 mm in length, respectively, to the forward end of the M115 primer. As shown in Figure 2, there were vent holes in the tube body and the tip. The vented primer tube was designed to locate the ignition source closer to the midsection of the propellant bed and to initially ignite more propellant so as to achieve more effective ignition. There were 2 and 4 $BKNO_3$ pellets inserted into the MK1 and MK2 primer tubes, respectively, to enhance the output of igniter gases. The resultant pressure-time traces obtained in the simulator diagnostics (Chang and Bonanno 1987) are displayed in Figure 3. The data show that an addition of the vented tube intruding into the propellant bed resulted in a substantial improvement in uniformity of the chamber pressure distribution during the early-phase interior ballistic cycle. Furthermore, in the diagnostics it was observed that the flamespreading along the propellant bed was significantly improved and the compaction of the bed was noticeably reduced. All of these are desired ignition characteristics which may lead to

good ballistic performance.

The objective of the present computer simulations is to examine the resultant ballistic performance from the three primer configurations and to compare two propelling charges of interest for their ballistic responses to primer configuration. In the simulations, the XKTC code is employed to take advantage of its two important features. One is that it permits the output rate of igniter gases to be specified as a function of time as well as location along the propellant bed. The other is its capability to account for intrusion of the projectile afterbody. In recent years, it has been suggested that gas-phase chemical kinetics may play an important role in the interaction between the combustion products of igniter material and the LOVA propellant (Keller and Horst 1987). However, the exact mechanism involved in the interaction remains unclear. Therefore, no consideration of finite-rate chemical kinetics is included in this work.

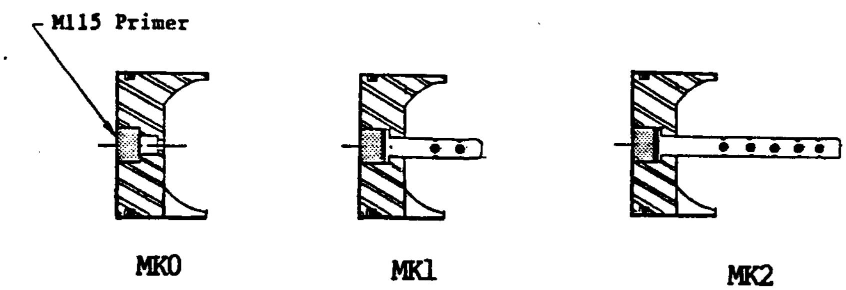

Figure 1. Primer Configurations.

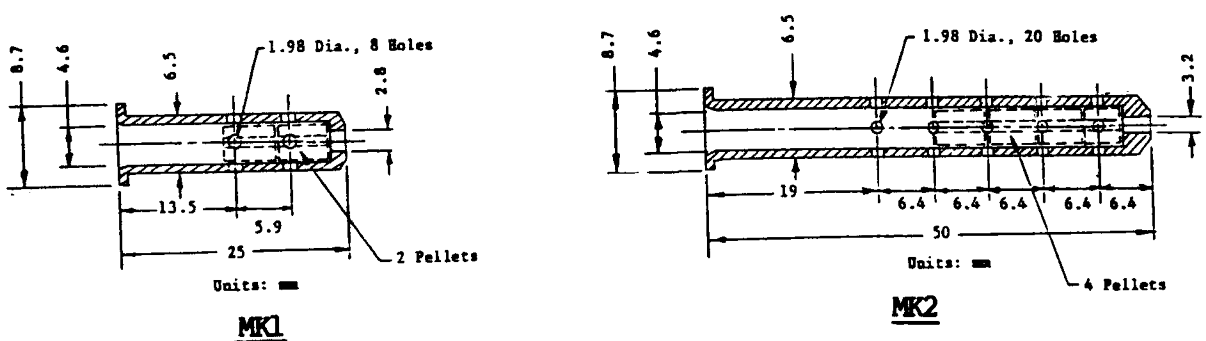

Figure 2. Vented Tubes in MK1 and MK2 Primers.

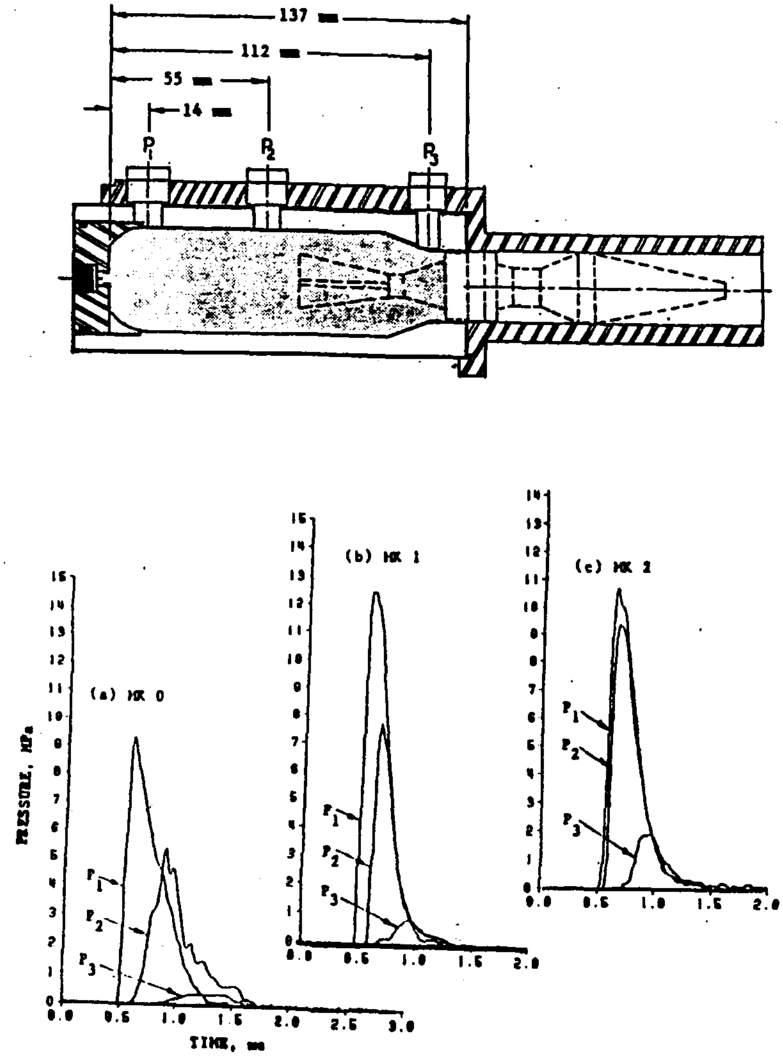

Figure 3. Pressure Data for LOVA Charges Fired in Gun Simulator at Ambient Temperature.

2. MODELING

2.1 Representation of Gun Chamber Configuration. Since the XKTC code simulates a one-dimensional flow with area change, some compromise in geometric aspects of the gun chamber is required. Figure 4 depicts both the actual (solid line) and the XKTC (dashed line) representations of the geometry. In the XKTC representation, the projectile fin assembly is compressed to a solid cylinder which has a volume identical to its original volume. Thus, the total chamber volume for gases and propellant remains unchanged.

2.2 Input Data. The input data for the XKTC code include the physical properties and internal dimensions of the gun tube, properties (chemical and physical) and dimensions of propellant grains, and output rate as well as venting distribution of igniter gases. Some of these data are given in the following.

2.2.1 Gun Data.

Type	25-mm (rifled)
Travel (cm)	186.7
Groove Diameter (mm)	26
Land Diameter (mm)	25
Charge Volume (cm^3)	94.06
XM881 Projectile Weight (grams)	126.2

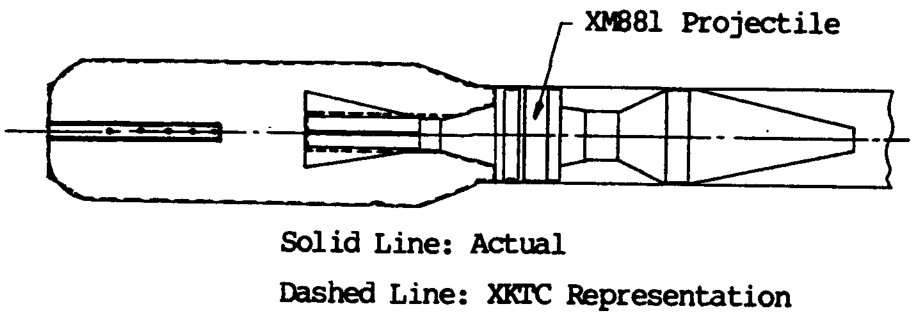

Figure 4. Geometrical Representation of Gun Chamber for XKTC Simulation.

2.2.2 Gun Bore Resistance. The bore resistance to the projectile motion down the gun tube is difficult to measure accurately. It is a function of a number of variables, such as the geometry and surface condition of the bore, geometry and mechanical properties of the actuator, and acceleration of the projectile. In the absence of experimental data, the values listed in Table 1 are determined by iteratively adjusting the bore resistance input into the computer code until the calculated maximum pressure at the breech and muzzle

velocity matched reasonably well with gun firing test results (see Subsection 3.1.1 for the matching case).

Table 1. Gun Bore Resistance

Distance From Breech		Bore Resistance	
(cm)	(inches)	(MPa)	(psi)
12.700	5.0	0.0	0.0
12.954	5.1	3.447	500.0
13.208	5.2	15.169	2200.0
13.716	5.4	16.203	2350.0
14.224	5.6	16.893	2450.0
38.100	15.0	3.448	500.0
198.120	78.0	0.689	100.0

2.2.3 Propellant Composition, Grain Dimensions, and Properties. Two kinds of propellants are considered in the present simulations: single-base (EXPRO Type 2164/2167) and nitramine composite HELP1. The composition of the single-base propellant is given in Table 2. The HELP1 propellant (lot 900-48, manufactured in the Naval Ordnance Station at Indian Head) is a high energy LOVA propellant which is one of the potential candidates for the 25-mm çannon system. Its composition is not given in this report due to classification. The grain dimensions and properties are listed in Table 3.

Table 2. Composition of the Single-Base Propellant

Name	Percentage Weight
NC(13.1%N)	93.883
MC	1.942
C	0.194
H2O	1.068
KS	0.971
ETOH	0.971
DPA	0.971

Table 3. Grain Dimensions and Properties

	Single-Base	HELP1
Density (g/cm^3)	1.6318	1.657
Outside Diameter (mm)	2.393	1.905
Perforation Diameter (mm)	0.1245	0.1524
Length (mm)	2.553	3.96
Number of perforations	7	7
Molecular Weight	24.022	21.71
Ratio of Specific Heats	1.2431	1.267
Covolume (cm^3/g)	1.0262	1.0969
Chemical Energy (cal/g)	973.5	1055.3

2.2.4 Burn Rates of Propellants.

Burn Rates From Closed Bomb Tests - see Table 4.

Table 4. Burn Rates From Closed Bomb Tests (cm/s)

Pressure		Single-Base		HELP1	
(MPa)	(kpsi)	(cm/s)	(in/s)	(cm/s)	(in/s)
13.79	2.0	1.351	0.532	0.406	0.16
20.68	3.0			0.737	0.29
34.47	5.0			1.956	0.77
62.06	9.0	4.65	1.8295		
68.95	10.0			4.902	1.93
137.90	20.0	12.353	4.8633		
172.37	25.0			8.585	3.38
275.80	40.0	23.641	9.3076		

Approximate Burn Rates for Calculations

In Figure 5, the solid triangles and solid circles are the data points tabulated in Table 4. The upper curve which closely fits the test data of the

single-base propellant is divided into three segments. The first segment is the region below 62.06 MPa, the second segment ranges from 62.06 MPa to 137.9 MPa, and the third segment is the region greater than 137.9 MPa. These three segments can be individually represented by three exponential functions in the following form

$$\text{Burn Rate (cm/s)} = aP^b$$

where a and b are constants and P is pressure in MPa. The values of "a" and "b" for the three functions are given in Table 5. The dashed line is an extrapolation of the segment in the low pressure region. For the HELP1 propellant, the data points from closed bomb tests in the low pressure region seem to be unrealistic. In fact, using these data computer simulations show that propagation of the flame through the propellant bed can not be sustained. This is because, after the peak of the primer output rate has passed, the amount of heat generated from the propellant ignition is less than the amount of heat dissipated. Strand burner tests for the propellant under controlled pressure values conducted by Miller at the BRL provide data represented by the open circles (Miller 1989). These data are drastically different from the

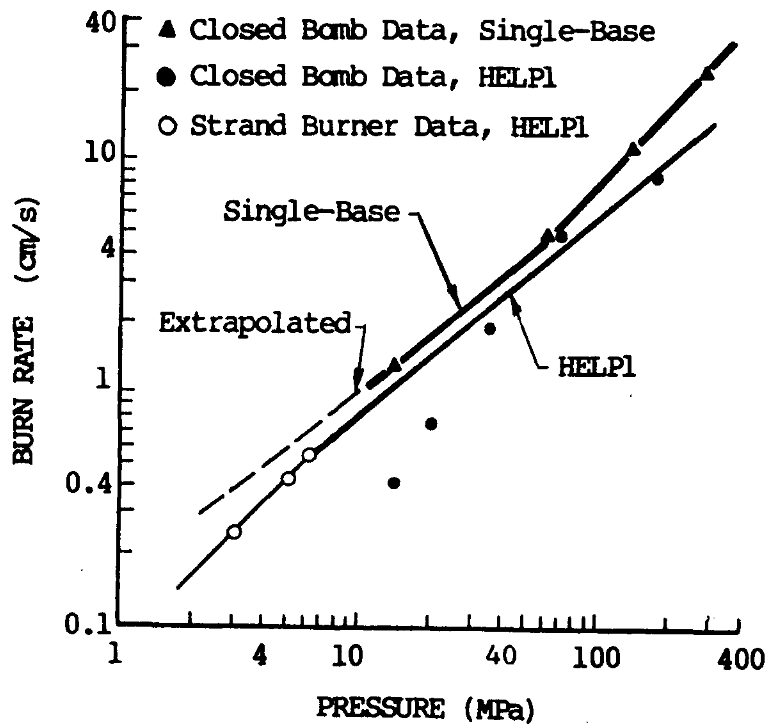

Figure 5. Propellant Burn Rates

closed bomb test results. It is believed that in the low pressure region the strand burner data are more reliable for the present calculations. The curve for HELP1 shown in the figure consists of two segments, each represented by the above exponential function with constants "a" and "b" given in Table 5.

2.2.5 Igniter Material and Output Rates of Igniter Gases. The igniter material in the M115 primer has a mass of 0.0999 gram and chemical energy of 605 cal/g. The $BKNO_3$ pellets inserted into the vented tubes in the MK1 and MK2 primers are single-perforation cylinders which have dimensions of 1.5 mm by 4 mm by 4.5 mm (inside diameter by outside diameter by length). Each pellet weighs 0.0422 gram and has chemical energy of 605.6 cal/g.

Table 6 lists the output rate of igniter combustion products at each location measured from the breech end at a prescribed time after the start of venting for each primer. These data are determined based on the total energy available in the primer and the duration of venting. Measurements from the simulator test (Chang and Bonanno 1987) show that the duration of venting of igniter gases was approximately 1.5 milliseconds. Observations on the MK1 and

Table 5. Approximate Burn Rates

Pressure Range		Single-Base			HELP1		
		a		b	a		b
(MPa)	(kpsi)	(cm/s)	(in/s)		(cm/s)	(in/s)	
< 62.06	< 9	0.54767	0.0010404	0.82067			
62.06 - 137.9	9 - 20	0.01385	0.0000263	1.22444			
> 137.9	> 20	0.24024	0.0004562	0.93647			
0.0 - 6.895	0 - 1				0.0776	0.0001474	1.07180
> 6.895	> 1				0.1143	0.0006019	0.86688

where < means "less than" and > means "greater than".

MK2 primers show that the venting along the vented segment of the primer tube was fairly uniform. In the table, it is noted that for the MK0 primer the venting site is specified from the breech end surface to a distance 0.95 cm away from the surface although there is no vented tube intruding into the propellant bed. This is because in reality the hot gases vented from the M115 primer can saturate the region covered by that range as observed in the simulator test with inert propellant grains in a size similar to that of live propellant grains (Chang and Bonanno 1987).

Table 6. Igniter Output Rate (g/cm-s)

Time (ms)	MK0 Primer 0.0*	.635*	.95*	MK1 Primer 1.27*	1.58*	1.90*	2.22*	2.54*
0.0	1047	1047	772	772	772	772	772	772
1.0	1047	1047	772	772	772	772	772	772
2.0	0.0	0.0	0.0	0.0	0.0	0.0	0.0	0.0

Time (ms)	MK2 Primer 1.25*	1.58*	2.54*	3.17*	3.81*	4.44*	5.08*
0.0	470	470	470	470	470	470	470
1.0	470	470	470	470	470	470	470
2.0	0.0	0.0	0.0	0.0	0.0	0.0	0.0

Note: The digits with * are the distances measured from the breech end, cm.

3. COMPUTATIONAL RESULTS

In the following, we first present the calculated results for the single-base charge with the XM881 projectile and the MK0 primer since the firing data for this round are available for validation. We then present the results for both the single-base and HELP1 charges with the MK1 and MK2 primers fired at ambient and -54°C.

3.1 Single-Base Charges.

3.1.1 At Ambient Temperature. Figure 6 shows the calculated pressure profile at the breech for the single-base propelling charge with the MK0 primer fired at ambient temperature. It matches well with the test result represented by the dashed line. In fact, the calculated muzzle velocity is only 1 m/s less than the value measured in the test firing.

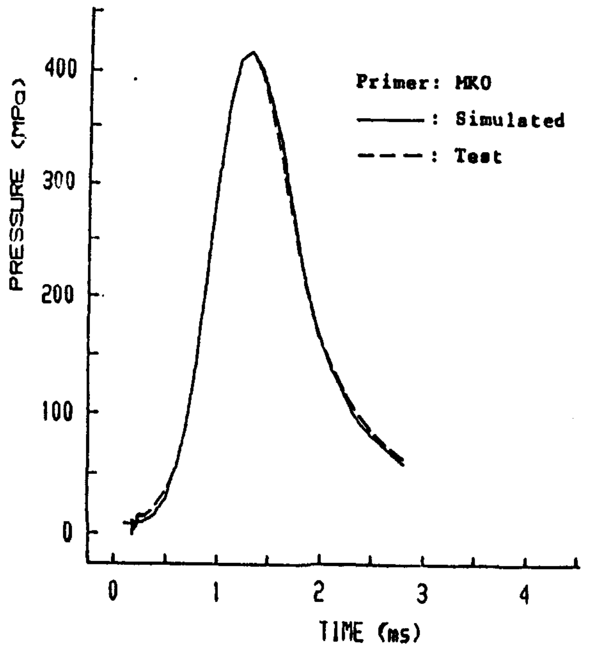

Figure 6. Breech Pressures: Tested and Simulated (Single-Base Charge)

Using the data base established for the bore resistance with this round, calculations were then performed for charges with the MK1 and MK2 primers. The results are given in Table 7. Plots are provided in Figures 7 through 15 for pressure, projectile velocity, projectile acceleration, mass fraction of unburned propellant, and flamespreading. Based on these data, a comparison of primer effectiveness for the three primer configurations are made as follows.

3.1.1.1 Pressure and Projectile Travel. In Table 7, we see that the peak pressure, P_{max}, increases progressively from the MK0 to the MK1 and to the MK2. Figure 7 provides a direct comparison of the pressure profiles at the breech. Apparently, the added vented tube in the MK1 and MK2 primers has

significantly increased the pressurization rate in the chamber, as a result of enhanced igniter output. This reduces the action time of the interior ballistic cycle from 2.81 milliseconds for the round with the MK0 primer to 2.58 milliseconds for the round with the MK2 primer. Figure 8 presents the same pressure rises at the breech as a function of projectile travel rather than time. This figure reveals that at the time the peak pressure arrives the projectile has traveled only 15-20 cm, which is 8-10% of the total projectile travel in the gun tube.

Table 7. Calculated Data for Single-Base Propelling Charges

Primer	Ch. Wt. (g)	Temp. (^{o}C)	P_{max} (MPa)	V_{muz} Inc. (%)	Mas. Fr.	F. Delay (ms)	Act. Time (ms)
MK0	93	amb.	417	0.0	.0012	.42	2.81
MK1	93	amb.	447	2.1	.0008	.35	2.69
MK2	93	amb.	485	3.8	.0005	.30	2.58
MK0	93	-54	392	0.0**	.0018	.53	2.92
MK1	93	-54	425	2.6**	.0011	.46	2.80
MK2	93	-54	463	4.3**	.0007	.42	2.69

Note: Ch. Wt. = total propelling charge weight.

P_{max} = peak pressure at the breech.

V_{muz} Inc. = percentage of increase in muzzle velocity over the muzzle velocity of the charge with the MK0 primer. Note that "**" is in reference to -54^{o}C rather than to ambient temperature. The actual muzzle velocities are not given due to the restriction of classification.

Mas. Fr. = mass fraction of unburned propellant at the time of shot exit.

F. Delay = time required for the flame front traveling to the forward end of the gun chamber.

Act. Time = total time elapsed from the start of venting of igniter gases to the time that the projectile exits the gun tube.

amb. = ambient temperature, 21^{o}C.

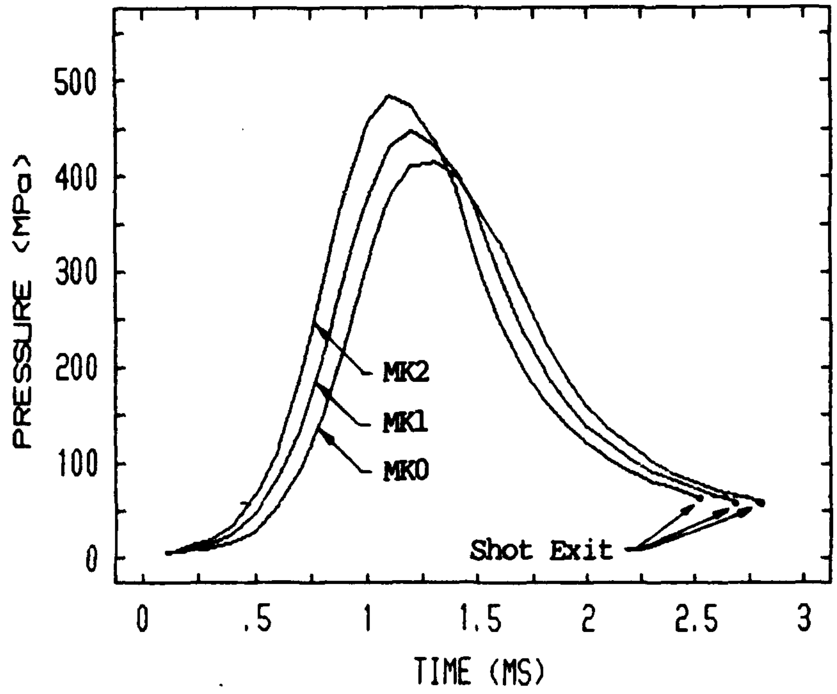

Figure 7. Breech Pressure vs. Time (Single-Base Charge).

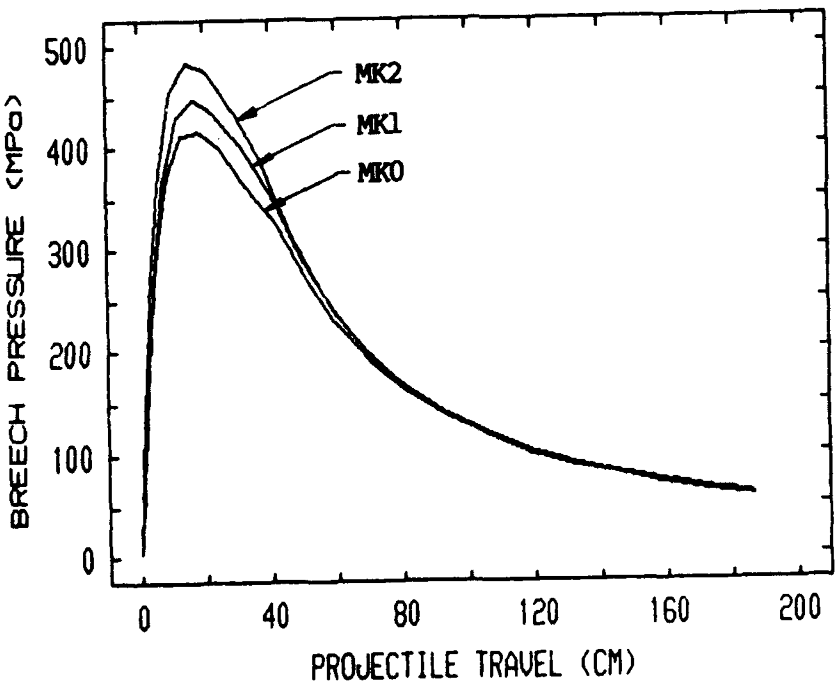

Figure 8. Breech Pressure vs. Projectile Travel (Single-Base Charge).

Figures 9 and 10 exhibit a series of pressure-time and pressure-projectile travel traces at locations of interest (breech, forward end of the gun chamber, and projectile base). In general, the pressure profiles are quite similar except that the peak pressures for the rounds with the MK1 and MK2 primers are higher. In Figure 9, dP is the value of the breech pressure minus the forward pressure in the gun chamber. The value can be of concern when it becomes a large negative value which is associated with "pressure waves" in the gun chamber. In the figures, the negative dP ranges from -6 MPa for the MK0 primer to -3 MPa for the MK2 primer, which are considered small values. The results in Figure 10 may be useful to the projectile designer. Maximum projectile base pressure is 71-72 % of the maximum breech pressure, and the pressure difference P between the breech and the projectile base can be more than 130 MPa.

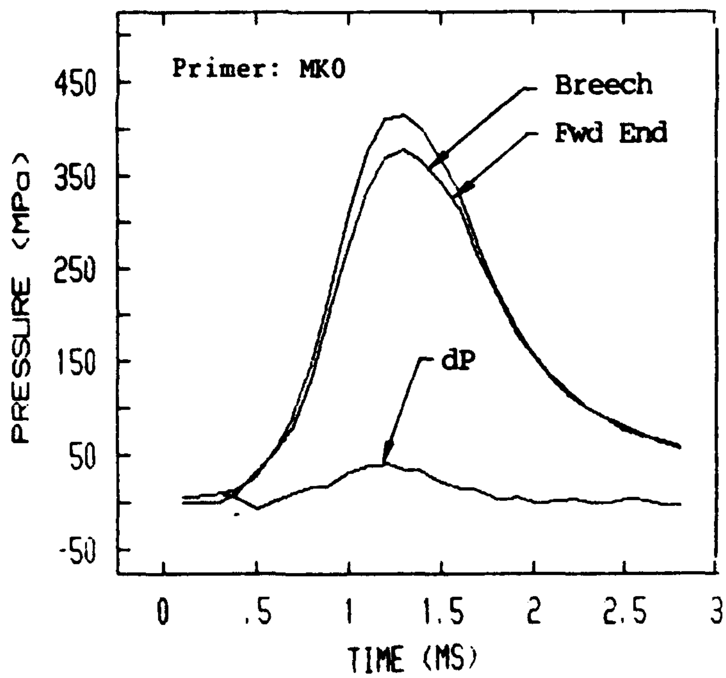

Figure 9. Pressures at Breech and Forward End of Gun Chamber and Their Differential (Single-Base Charge)

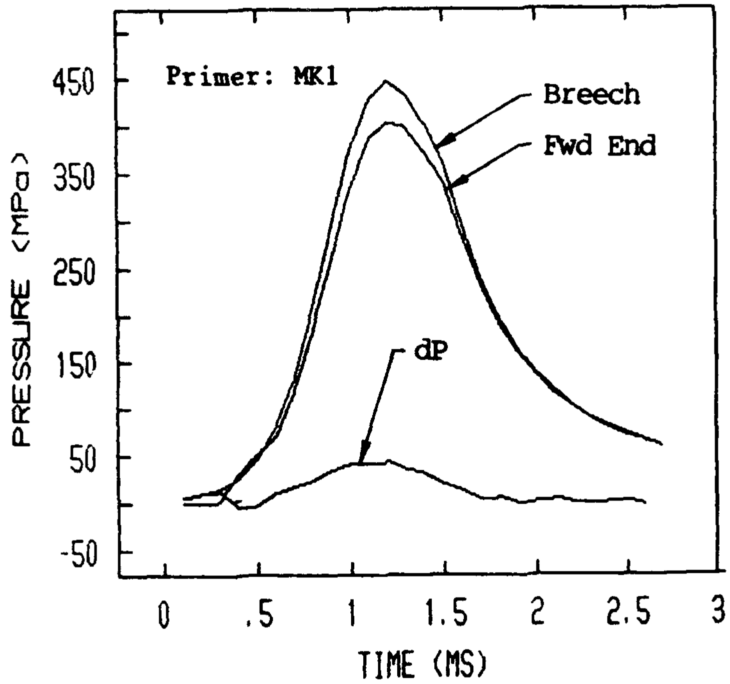

Figure 9. (Cont'd).

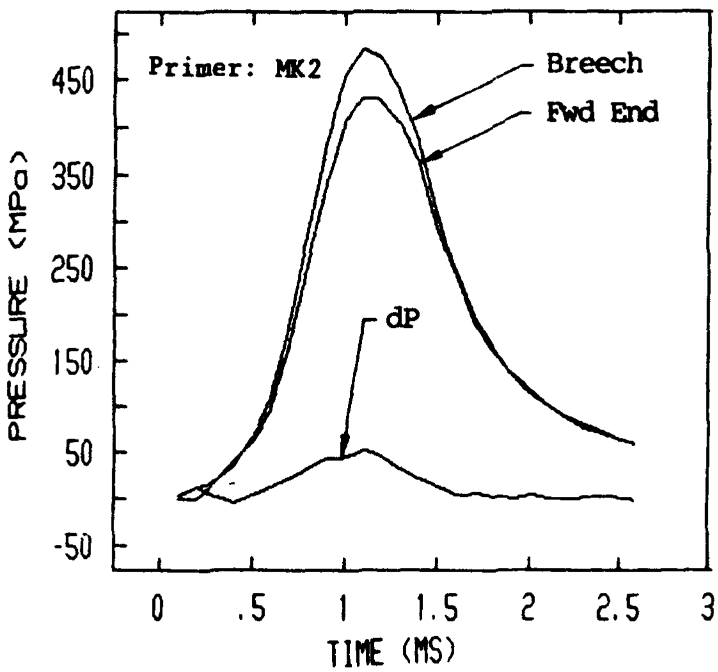

Figure 9. (Cont'd).

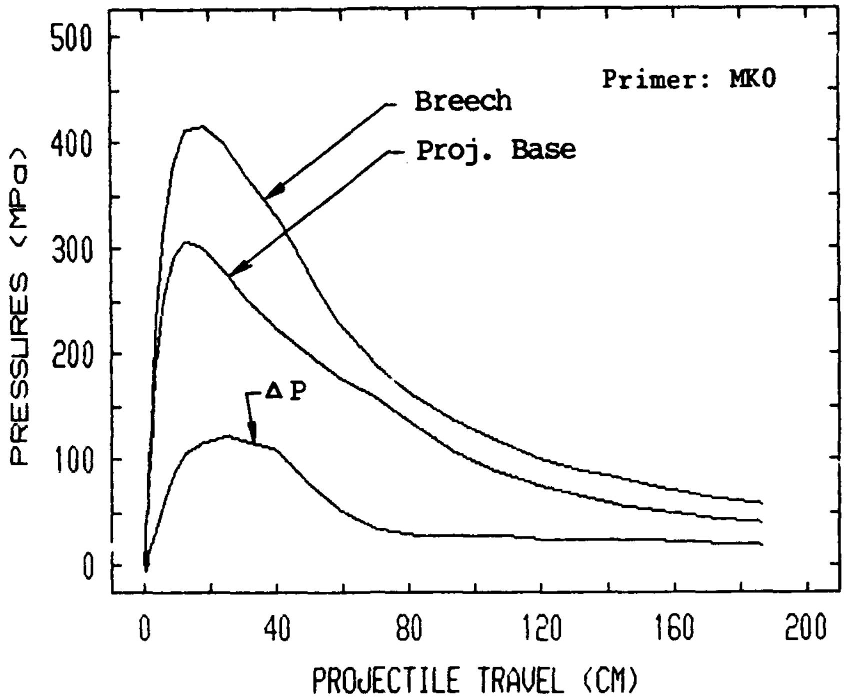

Figure 10. Pressures at Breech and Projectile Base and Their Differential (Single-Base Charge).

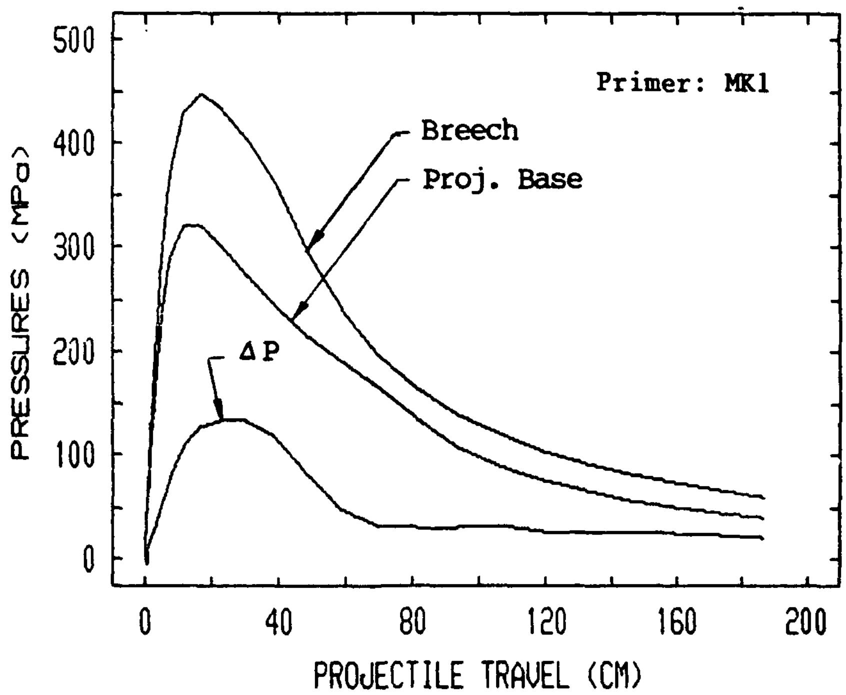

Figure 10. (Cont'd).

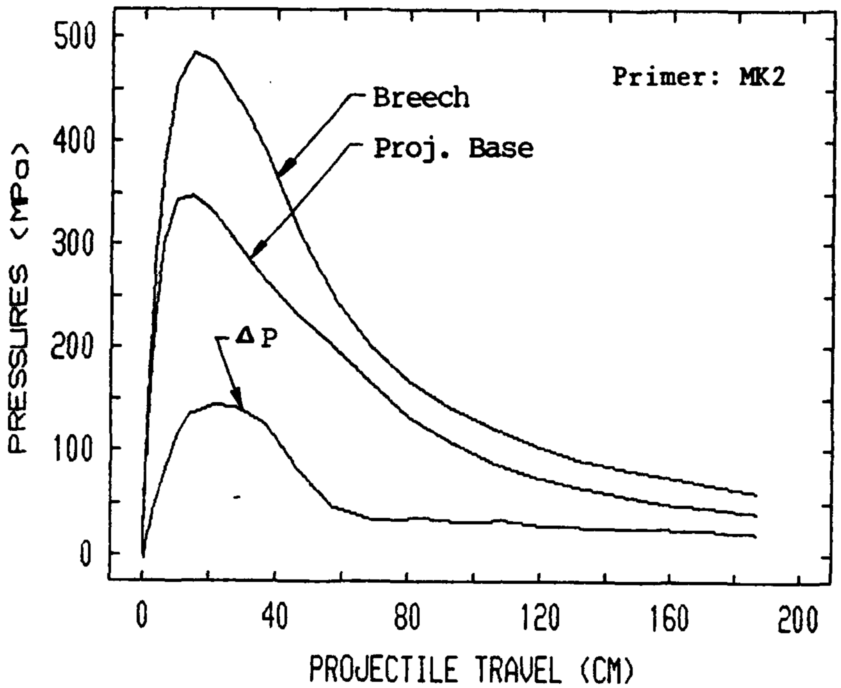

Figure 10. (Cont'd)

3.1.1.2 Projectile Acceleration. In Figure 11 the dashed lines represent projectile accelerations, showing that the MK2 primer results in the highest acceleration. As a result, the projectile velocity is increased by 3.8% over the round with the MK0 primer, as indicated in Table 7. It is noted that the maximum projectile acceleration occurs at the same projectile travel as the maximum breech pressure does. At this point, the projectile travel is about 17 cm which is 9% of the total projectile travel in the gun tube.

3.1.1.3 Mass Fraction of Unburned Propellant. Figure 12 is a plot of the unburned mass fraction of propellant versus projectile travel, showing that the mass is consumed very quickly in the first 20 cm of the projectile travel.

3.1.1.4 Flamespreading. Flamespreading in the propellant bed plays a key role in governing the interior ballistic cycle. Effectiveness of an ignition system is often characterized by its ability to achieve fast and uniform flamespreading, so that localized pressurization is avoided. Each of the three curves in Figure 13 shows the trace of the flame front from the start of venting of igniter gases. In the charge with the MK0 primer, the primer

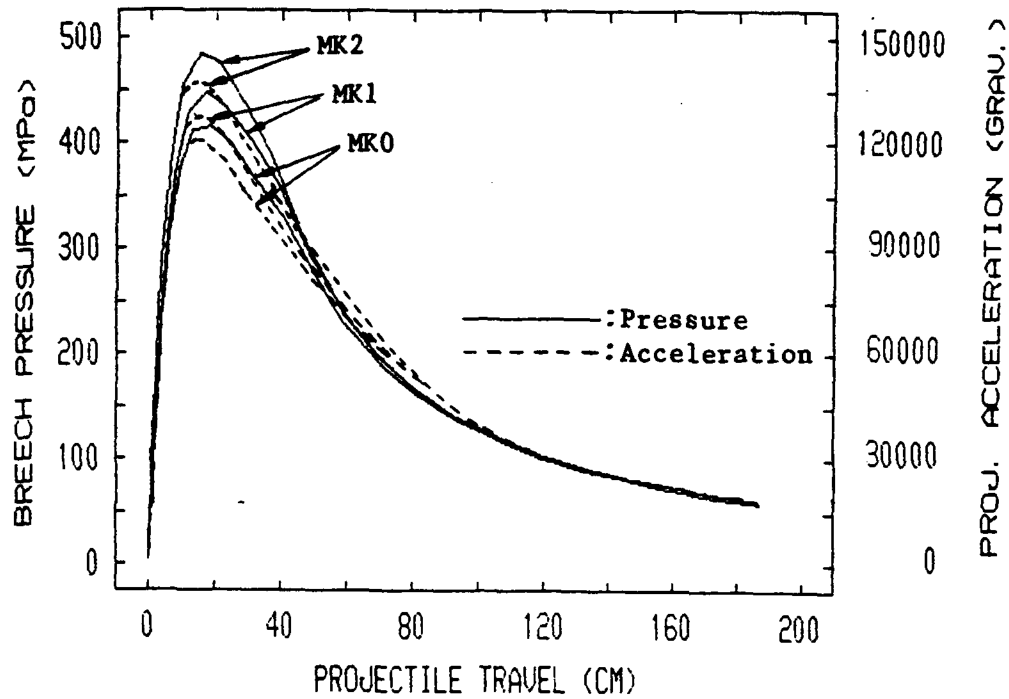

Figure 11. Breech Pressure and Projectile Acceleration (Single-Base Charge).

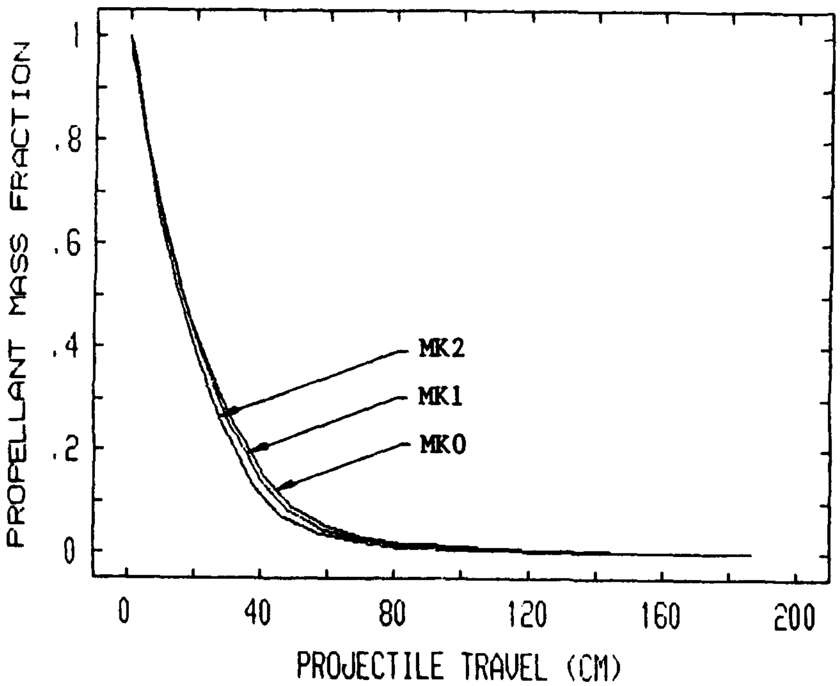

Figure 12. Propellant Mass Fraction vs. Projectile Travel (Single-Base Charge).

direction toward the forward end of the chamber. In the charge with the MK1 primer, the primer output is distributed over the vented segment of the primer tube, which ranges from 1 cm to 2.5 cm from the breech end. Flame should uniformly cover that range following the functioning of the primer. In the figure, however, instead of a straight line, the curve appears to be highly irregular in that range. This behavior does not seem realistic and likely results from the numerical solution of the present one-dimensional flow computer code. When treated as a one-dimensional flow, there is a stagnation region in the mid-section of the vented primer tube during the very early period of flamespreading. In this region, there is no convective heating to the propellant and, therefore, there is a delay of flamespreading as shown in the figure. Immediately after its appearance, the flame spreads in two directions: one toward the breech end and the other toward the forward end of the chamber. In the case of using MK2 primer which has a longer vented tube, the initial flame coverage is even larger. A comparison of the three curves clearly indicates that a long primer tube can significantly reduce the flamespread delay.

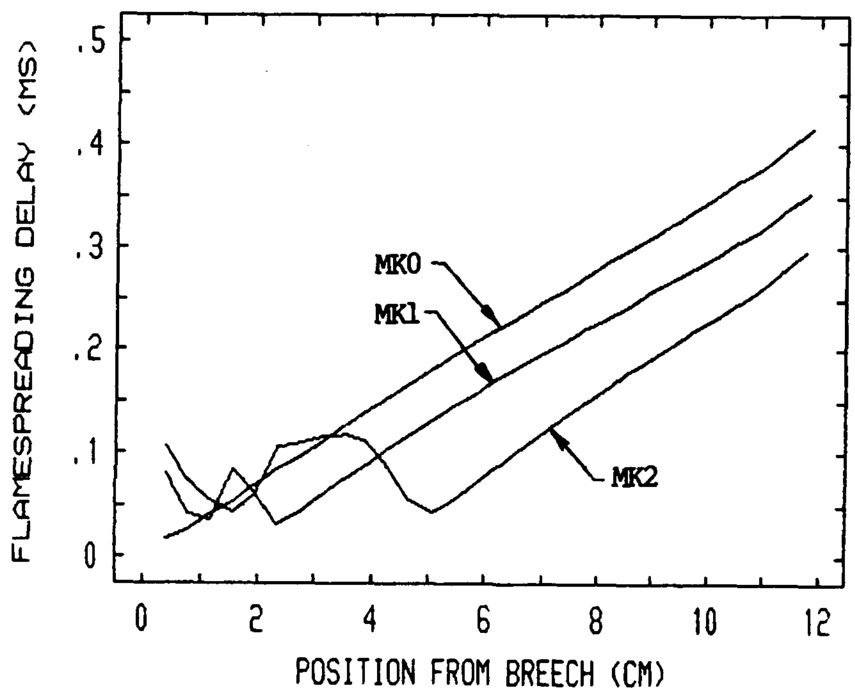

Figure 13. Flamespread Delay (Single-Base Charge)

In Figure 14, we have noticed an interesting correlation between the flamespreading and the early pressure rise at the breech. The correlation is that rapid flamespreading results in a rapid pressure rise. However, this correlation may not necessarily be true in large ammunition, where in the case of localized ignition near the breech, the breech pressure may rise very rapidly in spite of slow flamespreading. In the figure we also have noticed that at the time the flame reaches the forward end of the chamber, the pressures for all of the three primers have reached almost the same level, 25 MPa, as indicated by the dashed lines.

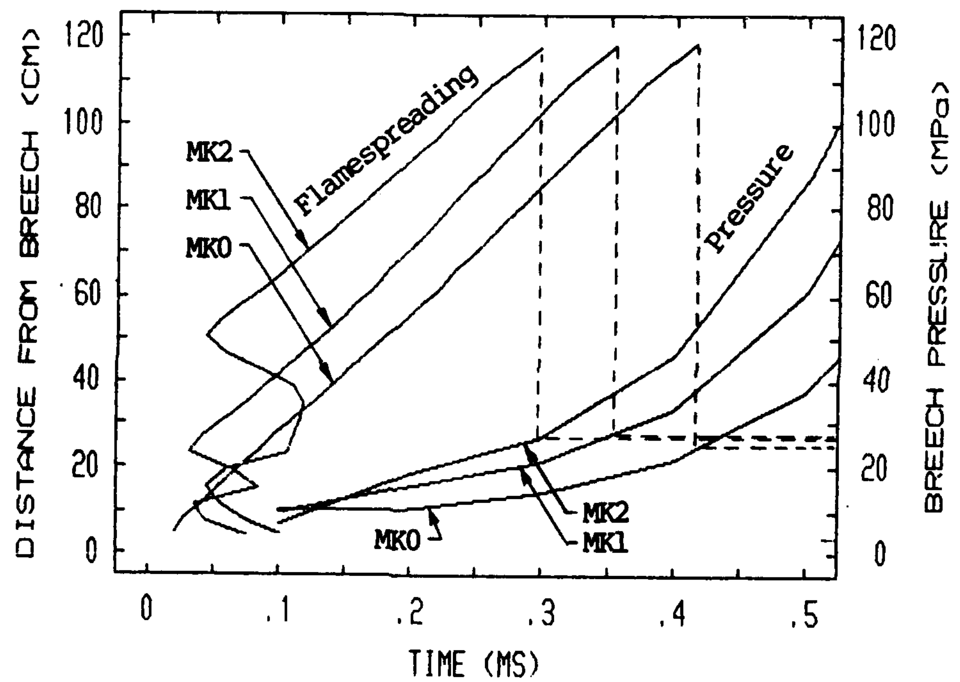

Figure 14. Correlation Between Flamespread Delay and Breech Pressure Rise (Single-Base Charge).

In the simulator tests (Chang and Bonanno 1987) with the MK0 primer, a charge weight of 93 grams would fill the chamber leaving no ullage. This is the same charge weight used in the gun firing tests. When subjected to vibrations, the same charge weight would also fill in the rounds with the MK1 and MK2 primers. In addition to using 93 grams, XKTC simulations were carried out for the rounds with a reduced charge weight to account for the volume occupied by the added primer tubes. The resultant charge weights are 92.4

grams and 91.6 grams for the rounds with the MK1 primer and MK2 primer, respectively. In Table 8, the results show that even at a reduced charge weight there is still a noticeable improvement in muzzle velocity for rounds using the MK1 and MK2 primers over the MK0 primer. It is believed that the consistency of ballistic performance in actual firings can be improved in using the MK1 and MK2 primers.

Table 8. Calculated Data for Single-Base Propelling Charges at Reduced Charge Weights

Primer	Ch. Wt. (grams)	Temp. (^{o}C)	P_{max} (MPa)	V_{muz} Inc. %	Mas. Fr.	F. Delay (ms)	Act. Time (ms)
MK0	93.0	amb.	417	0.0	.0012	.42	2.81
MK1	92.4	amb.	435	1.4	.0009	.35	2.72
MK2	91.6	amb.	452	2.0	.0008	.24	2.56

Note: V_{muz} Inc. = percentage of increase in muzzle velocity over the muzzle velocity of the charge with the MK0 primer.

3.1.2 At -54°C (-65°F). The results for the rounds at -54°C are also given in Table 7. As expected, both the peak pressure and muzzle velocity drop to some extent in comparison to the values for ambient temperature. The mass fraction of unburned propellant at shot exit is increased. Furthermore, the ballistic action time is longer. All of these data are the indication of a slower and less complete combustion process occurring in the cold rounds. We also note that there is a larger difference in muzzle velocity from using one kind of primer to the another in the rounds at a cold temperature than at ambient temperature. For instance, at ambient temperature the velocity increase for the MK2 primer over the MK0 primer is 3.8%, while at -54°C the increase is 4.3%. The implication is that at cold temperatures, the ballistic performance is more sensitive to the primer configuration. Thus, for cold rounds there is a stronger need to use a highly effective ignition system in order to achieve required ballistic performance.

3.2 HELP1 Charges. Following the same procedure as for the single-base charges, calculations were carried out for HELP1 charges using the three primer configurations. Results obtained are listed in Table 9 and plotted in Figures 15 through 17. At either ambient temperature or -54°C, both the peak pressure at the breech and the muzzle velocity increase progressively from the charge using the MK0 primer to the charge using the MK2 primer. The mass fraction of unburned propellant and the action time of the ballistic cycle, both decrease in the rounds using MK1 and MK2 primers. Again, the indication is that the overall ballistic performance has been influenced by the selection of primer configuration, as seen earlier in the single-base propelling charges.

Table 9. Calculated Data for HELP1 Propelling Charges

Primer	Ch. Wt. (grams)	Temp. (°C)	P_{max} (MPa)	V_{muz} Inc. (%)	Mas. Fr.	F. Delay (ms)	Act. Time (ms)
MK0	93	amb.	401	0.0	.0076	.45	2.73
MK1	93	amb.	427	2.4	.0059	.39	2.62
MK2	93	amb.	461	4.1	.0047	.35	2.54
MK0	93	-54	377	0.0**	.0090	.55	2.84
MK1	93	-54	405	3.3**	.0063	.50	2.71
MK2	93	-54	444	4.9**	.0052	.45	2.63

Note: "**" is in reference to -54°C rather than to ambient temperature.

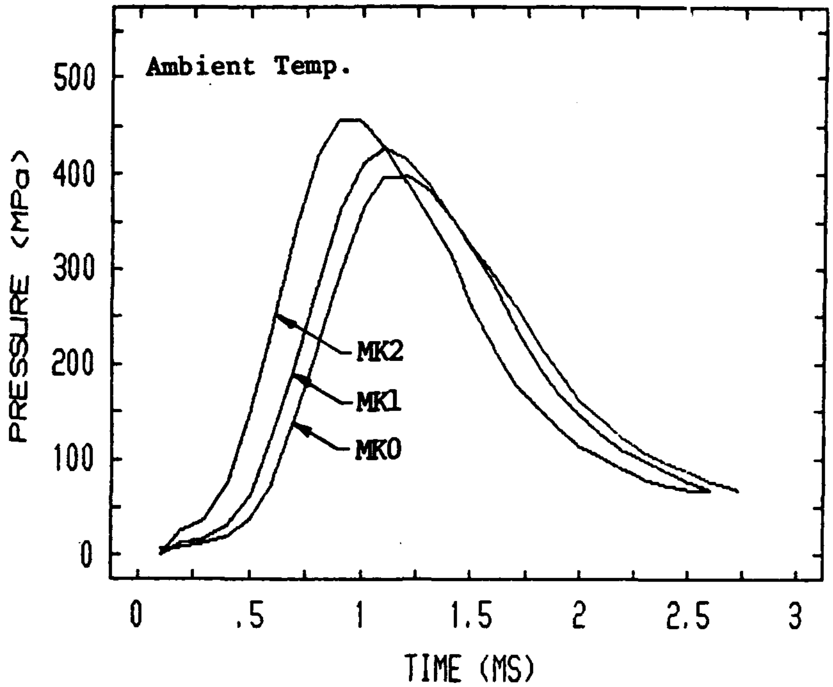

Figure 15. Breech Pressure vs. Time (HELP1 Charge).

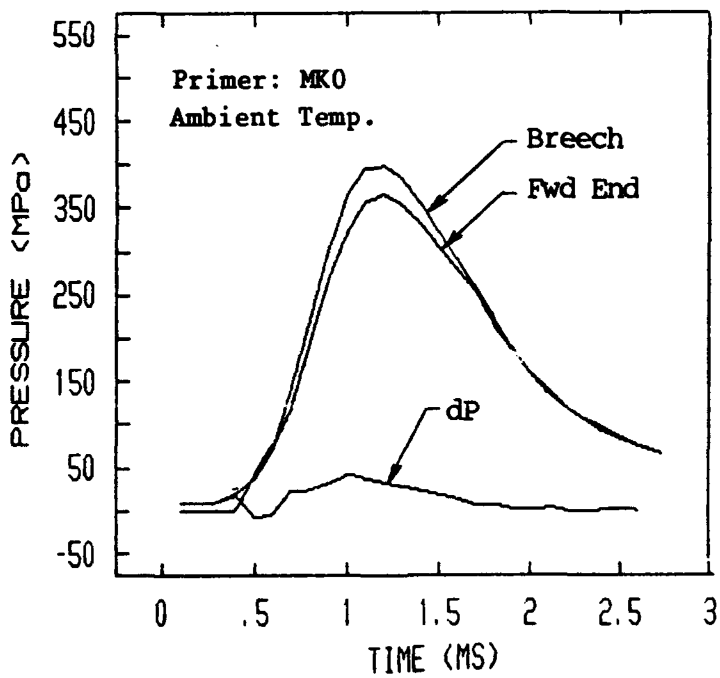

Figure 16. Pressures at Breech and Forward End of Gun Chamber and Their Differential (HELP1 Charge).

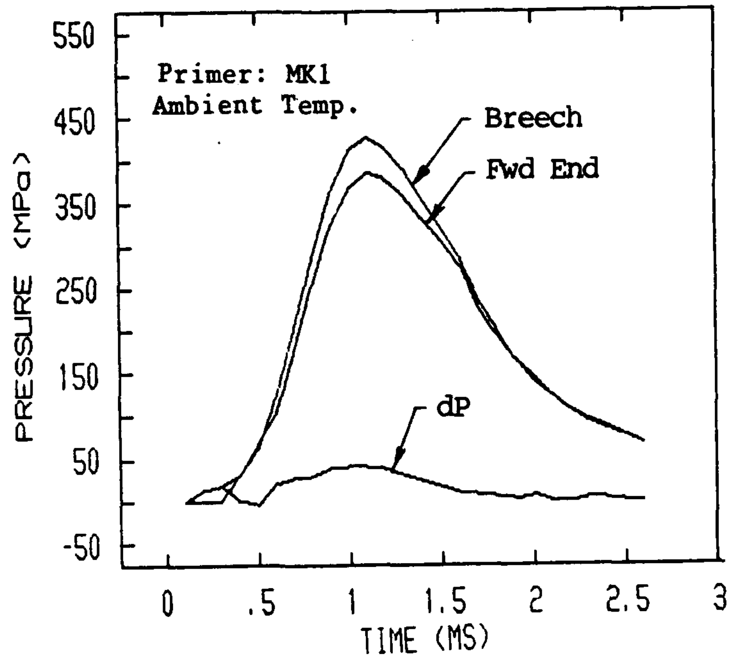

Figure 16. (Cont'd).

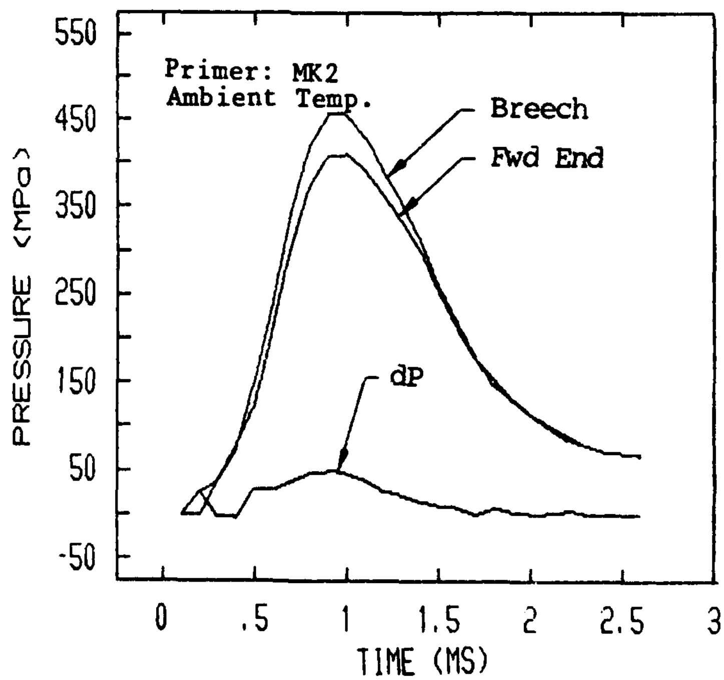

Figure 16. (Cont'd).

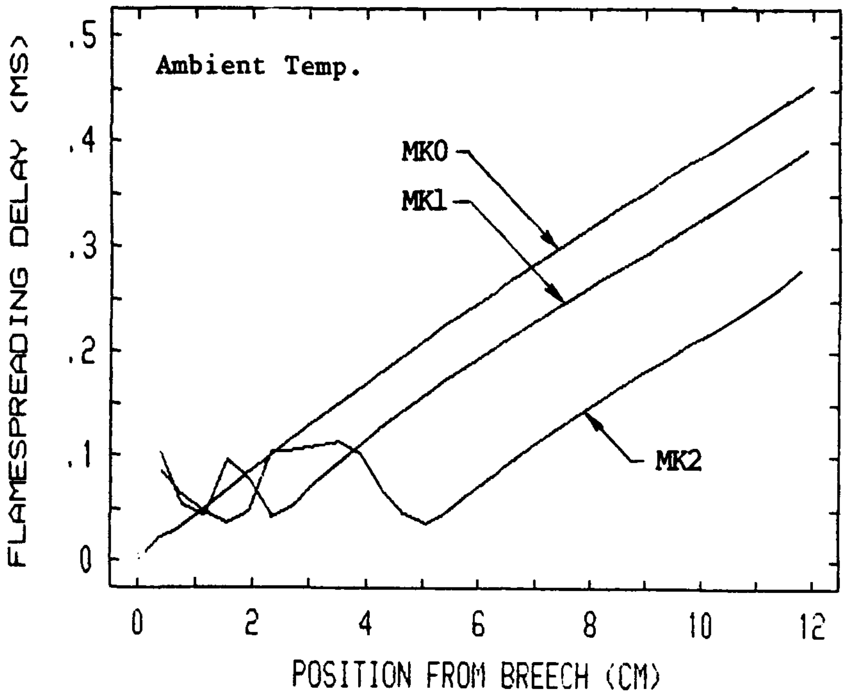

Figure 17. Flamespread Delay (HELP1 Charge).

3.3 Comparison of Ballistic Performance Between the Single-Base Charge and the HELP1 Charge. In comparing Table 7 with Table 9 for the calculated data, several different characteristics of interest between the single-base propellant and the HELP1 propellant are noticed as follows.

o Using the same primer configuration the P_{max} is lower for the HELP1 charge; however, the muzzle velocity is higher. This may be explained as a result of a lower burn rate (see Figure 5) but a higher energy for the HELP1 propellant.

o The flamespread delay for the HELP1 charge is longer, but its ballistic action time turns out to be shorter. The longer flamespread delay is attributed to a higher ignition temperature (in the calculations, the temperature inputs are $850^{o}R$ for the HELP1 propellant and $800^{o}R$ for the single-base propellant) and a lower burn rate. The shorter ballistic action time seems to be a result of its higher energy.

o The improvement of ballistic performance by using the MK1 and MK2 primers over the MK0 primer is greater for the HELP1 charge, implying that the HELP1 charge is more sensitive to the selection of primer configuration.

3.4 <u>Effects of Primer Output Rate on Ballistic Performance</u>. It is expected that an increase in the output rate of igniter gases will reduce the ignition delay of propellant. Nevertheless, it is unknown whether the increase will result in a higher chamber pressure and a greater muzzle velocity in the charges under consideration for the 25-mm gun system. The answer is of interest to charge developers. We select the MK2 primer for investigation because the primer permits a wider variation of the number of $BKNO_3$ pellets to be inserted. Table 10 presents results for both the single-base and the HELP1 charges in which the number of $BKNO_3$ pellets varies from 2 to 8. Surprisingly, the table shows that the variation produces little change in P_{max} and muzzle velocity. For an explanation, we note in Figure 18 that the pressurization rate (i.e. the quickness of pressure rise) in the early stage of the interior ballistic cycle increases with the number of $BKNO_3$ pellets.

Table 10. <u>Effects of Weight Variation of Igniter Material</u>

Prop.	Primer	No. of Pellets	Ch. Wt. (grams)	Pmax (MPa)	Vmuz Inc. (%)	Mas. Fr.	F. Delay (ms)	Act. Time (ms)
S-B	MK0	0	93	417	0.0	.0012	.42	2.81
S-B	MK2	2	93	486	3.8	.0005	.37	2.67
S-B	MK2	4	93	485	3.8	.0005	.30	2.58
S-B	MK2	6	93	484	3.8	.0006	.26	2.54
S-B	MK2	8	93	484	3.8	.0006	.24	2.50
HELP1	MK0	0	93	401	0.0	.0076	.45	2.73
HELP1	MK2	2	93	462	4.2	.0046	.44	2.64
HELP1	MK2	4	93	461	4.2	.0047	.35	2.54
HELP1	MK2	6	93	459	4.2	.0049	.30	2.47
HELP1	MK2	8	93	459	4.2	.0050	.28	2.44

where S-B = single-base.

As a result, projectile motion takes place earlier in the case with more $BKNO_3$ pellets. The earlier projectile motion produces an increased chamber volume behind the projectile and thus the maximum chamber pressure does not increase

with the number of $BKNO_3$ pellets inserted. However, these results may not be true for a large caliber tank charge, such as the 105-mm and 120-mm systems, in light of its much larger and much longer propellant bed.

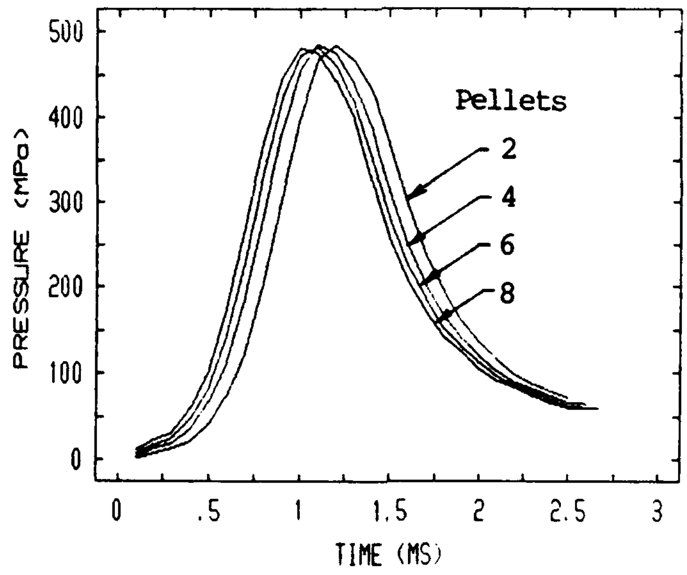

Figure 18. Effect of Primer Output Rate on Breech Pressure (Single-Base Charge).

4. CONCLUSIONS

Calculated results for the single-base and HELP1 charges at ambient and -54°C show that the addition of a vented primer tube intruding into the propellant bed improves the muzzle velocity and reduces the action time of the interior ballistic cycle. This correlates well with the previous experimental results that the primer tube improves the uniformity of pressure distribution and the flamespreading along the propellant bed in the early ignition phase; the longer the primer tube, the better improvement in muzzle velocity.

There are differences in ballistic characteristics between the conventional single-base propellant and the nitramine composite HELP1 propellant considered. Typically, (1) flamespreading is slower in the HELP1 charge and (2)

of primer configuration.

For both charges, single-base and HELP1, the ballistic performance is more sensitive to primer configuration when they are at -54°C than at ambient temperature.

An increase in the MK2 primer output rate does not influence the peak pressure and the muzzle velocity in the charges studied. However, the action time of the interior ballistic cycle is noticeably reduced.

Some other results of interest are noted as follows:

- o Maximum breech pressure -- occurs when the projectile travels 15-20 cm from the breech end (8-10% of the total projectile travel in the gun tube).
- o Maximum projectile base pressure -- is about 72% of the maximum breech pressure.
- o Propellant mass fraction -- unburned propellant mass decreases very rapidly during the first 20 cm of projectile travel.

INTENTIONALLY LEFT BLANK.

5. REFERENCES

Chang, L. M., and A. Bonanno. "Ignition Studies of Prototype Low-Vulnerability Charges for the 25-mm Gun System." 1987 JANNAF Combustion Meeting, CPIA Publication 476, Vol. III, October 1987.

Gough, P.S. "The XNOVAKTC Code." BRL-CR-627, U.S. Army Ballistic Research Laboratory, Aberdeen Proving Ground, MD, February 1990.

Keller, G.E., and A. W. Horst. "The Two Phase Flow Simulation of LOVA Propellant Interior Ballistic Behavior Using the XNOVAK Code." BRL-TR-2796, U.S. Army Ballistic Research Laboratory, Aberdeen Proving Ground, MD, April 1987.

Miller, M.S. Private communication, February 1989.

INTENTIONALLY LEFT BLANK.

No. of Copies	Organization
2	Administrator Defense Technical Info Center ATTN: DTIC-DDA Cameron Station Alexandria, VA 22304-6145
1	Commander U.S. Army Materiel Command ATTN: AMCAM 5001 Eisenhower Ave. Alexandria, VA 22333-0001
1	Commander U.S. Army Laboratory Command ATTN: AMSLC-DL 2800 Powder Mill Rd. Adelphi, MD 20783-1145
2	Commander U.S. Army Armament Research, Development, and Engineering Center ATTN: SMCAR-IMI-I Picatinny Arsenal, NJ 07806-5000
2	Commander U.S. Army Armament Research, Development, and Engineering Center ATTN: SMCAR-TDC Picatinny Arsenal, NJ 07806-5000
1	Director Benet Weapons Laboratory U.S. Army Armament Research, Development, and Engineering Center ATTN: SMCAR-CCB-TL Watervliet, NY 12189-4050
(Unclass. only)1	Commander U.S. Army Armament, Munitions, and Chemical Command ATTN: AMSMC-IMF-L Rock Island, IL 61299-5000
1	Director U.S. Army Aviation Research and Technology Activity ATTN: SAVRT-R (Library) M/S 219-3 Ames Research Center Moffett Field, CA 94035-1000
1	Commander U.S. Army Missile Command ATTN: AMSMI-RD-CS-R (DOC) Redstone Arsenal, AL 35898-5010

No. of Copies	Organization
1	Commander U.S. Army Tank-Automotive Command ATTN: ASQNC-TAC-DIT (Technical Information Center) Warren, MI 48397-5000
1	Director U.S. Army TRADOC Analysis Command ATTN: ATRC-WSR White Sands Missile Range, NM 88002-5502
1	Commandant U.S. Army Field Artillery School ATTN: ATSF-CSI Ft. Sill, OK 73503-5000
2	Commandant U.S. Army Infantry School ATTN: ATZB-SC, System Safety Fort Benning, GA 31903-5000
(Class. only)1	Commandant U.S. Army Infantry School ATTN: ATSH-CD (Security Mgr.) Fort Benning, GA 31905-5660
(Unclass. only)1	Commandant U.S. Army Infantry School ATTN: ATSH-CD-CSO-OR Fort Benning, GA 31905-5660
1	WL/MNME Eglin AFB, FL 32542-5000
	<u>Aberdeen Proving Ground</u>
2	Dir, USAMSAA ATTN: AMXSY-D AMXSY-MP, H. Cohen
1	Cdr, USATECOM ATTN: AMSTE-TC
3	Cdr, CRDEC, AMCCOM ATTN: SMCCR-RSP-A SMCCR-MU SMCCR-MSI
1	Dir, VLAMO ATTN: AMSLC-VL-D
10	Dir, USABRL ATTN: SLCBR-DD-T

No. of Copies	Organization
1	OSD/SDIO/IST ATTN: Dr. Len Caveny Pentagon Washington, DC 20301-7100
1	Commander U.S. Army Concepts Analysis Agency ATTN: D. Hardison 8120 Woodmont Ave. Bethesda, MD 20014-2797
1	Commander, USACECOM R&D Technical Library ATTN: ASQNC-ELC-IS-L-R, Myer Center Fort Monmouth, NJ 07703-5301
9	Commander U.S. Army Armament, Research, Development and Engineering Center ATTN: SMCAR-AEE-B, A. Beardell D. Downs S. Einstein S. Westley S. Bernstein J. Rutkowski B. Brodman SMCAR-AES, D. Spring S. Kaplowitz Picatinny Arsenal, NJ 07801-5000
2	Commander U.S. Army Armament, Research, Development and Engineering Center ATTN: SMCAR-HFM, E. Barrieres R. Davitt Picatinny Arsenal, NJ 07801-5000
1	Commander U.S. Army Armament, Research, Development and Engineering Center ATTN: SMCAR-CCH-V, C. Mandala Picatinny Arsenal, NJ 07801-5000

No. of Copies	Organization
1	Commander U.S. Army Armament, Research, Development and Engineering Center ATTN: SMCAR-FSA-T, M. Salsbury Picatinny Arsenal, NJ 07801-5000
1	Commander U.S. Army TSARCOM 4300 Goodfellow Boulevard St. Louis, MO 63120-1702
1	Commander U.S. Army Harry Diamond Laboratories ATTN: SLCHD-TA-L 2800 Powder Mill Road Adelphi, MD 20783-1145
1	Commander U.S. Army Research Office ATTN: Technical Library P.O. Box 12211 Research Triangle Park, NC 27709-2211
1	Commander U.S. Army Belvoir Research and Development Center ATTN: STRBE-WC Fort Belvoir, VA 22060-5006
3	Commander Radford Army Ammunition Plant ATTN: SMCAR-QA/HI LIB Radford, VA 24141-0298
1	Commander U.S. Army Foreign Science and Technology Center ATTN: AMXST-MC-3 220 Seventh St., NE Charlottesville, VA 22901-5396
1	Commander U.S. Army Material Command ATTN: AMCPM-DW 5001 Eisenhower Ave. Alexandria, VA 22333-5001

No. of Copies	Organization
1	Department of the Army Office of the Product Manager 155-mm Howitzer, M109A6, Paladin ATTN: SFAE-AR-HIP-IP, Mr. R. De Kleine Picatinny Arsenal, NJ 07806-5000
1	Director HQ, TRAC RPD ATTN: ATRC, MAJ Williams Fort Monroe, VA 23651-5143
1	Director U.S. Army Materials Technology Laboratory ATTN: SLCMT-ATL Watertown, MA 02172-0001
1	Commandant U.S. Army Aviation School ATTN: Aviation Agency Fort Rucker, AL 36360
1	Commandant U.S. Army Special Warfare School ATTN: Rev & Tng Lit Division Fort Bragg, NC 28307
1	Commandant U.S. Army Field Artillery School ATTN: ATSF-SCI Fort Sill, OK 73503-5660
1	Commandant U.S. Army Command and General Staff College Fort Leavenworth, KS 66027
1	Commandant U.S. Army Armor School ATTN: ATZK-CD-MS, M. Falkovitch Armor Agency Fort Knox, KY 40121-5215

No. of Copies	Organization
1	Director U.S. Army TRAC-Fort Lee ATTN: ATRC-L, Mr. Cameron Fort Lee, VA 23801-6140
1	Commander U.S. Army Ballistic Missile Defense System Command Advanced Technology Center P.O. Box 1500 Huntsville, AL 35807-3801
1	President U.S. Army Artillery Board Fort Sill, OK 73503-5600
1	Project Manager U.S. Army Tank-Automotive Command Improved TOW Vehicle ATTN: AMCPM-ITV Warren, MI 48397-5000
1	Project Manager U.S. Army Tank-Automotive Command Fighting Vehicle Systems ATTN: AMCPM-BFVS Warren, MI 48092-2498
1	Project Manager Abrams Tank System ATTN: SFAE-ASM-AB Warren, MI 48397-5000
2	Project Manager U.S. Army Tank-Automotive Command ATTN: SFAE-ASM-SS-T, T. Dean (2 cp) Warren, MI 48092-2498
2	Commander Naval Sea Systems Command ATTN: SEA 62R SEA 64 Washington, DC 20362-5101
1	Commander Naval Air Systems Command ATTN: AIR-954-Technical Library Washington, DC 20360

No. of Copies	Organization
5	Commander Naval Surface Weapons Center ATTN: Code G33, J. L. East W. Burrell J. Johndrow Code G23, D. McClure Code DX-21 Technical Library Dahlgren, VA 22448-5000
4	Commander Naval Surface Weapons Center ATTN: Code 240, S. Jacobs Code 730 Code R-13, K. Kim R. Bernecker Silver Springs, MD 20903-5000
2	Commanding Officer Naval Underwater Systems Center Energy Conversion Dept. ATTN: Code 5B331, R. S. Lazar Technical Library Newport, RI 02840
1	Assistant Secretary of the Navy (R, E, and S) ATTN: R. Reichenbach Room 5E787 Pentagon Building Washington, DC 20350
1	Office of Naval Research ATTN: Code 473, R. S. Miller 800 N. Quincy St. Arlington, VA 22217-9999
2	Commander U.S. Naval Surface Weapons Center ATTN: J. P. Consaga C. Gotzmer Indian Head, MD 20640-5000

No. of Copies	Organization
3	Commander Naval Weapons Center ATTN: Code 388, C. F. Price T. Parr Info. Sci. Div China Lake, CA 93555-6001
1	Director Naval Research Laboratory ATTN: Technical Library Washington, DC 20375
3	AL/LSCF ATTN: J. Levine L. Quinn T. Edwards Edwards Air Force Base, CA 93523-5000
1	AT/TSTL (Tech Library) ATTN: J. Lamp Edwards Air Force Base, CA 93523-5000
1	AFATL/DLYV Eglin Air Force Base, FL 32542-5000
1	AFATL/DLXP Eglin Air Force Base, FL 32542-5000
1	AFATL/DLJE Eglin Air Force Base, FL 32542-5000
2	Director Lawrence Livermore National Laboratory ATTN: L-355, A. Buckingham M. Finger P.O. Box 808 Livermore, CA 94550-0622
1	Director Lawrence Livermore National Laboratory ATTN: L-324, M. Constantino P.O. Box 808 Livermore, CA 94550-0622

No. of Copies	Organization
1	Princeton Combustion Research Laboratory Inc. ATTN: M. Summerfield 475 U.S. Highway One Monmouth Junction, NJ 08852-9650
1	Central Intelligence Agency 01R/DB/Standard Washington, DC 20505
1	University of Massachusetts Dept. of Mechanical Engineering ATTN: K. Jakus Amherst, MA 01002-0014
1	Brigham Young University Dept of Chemical Engineering ATTN: M. Beckstead Provo, UT 84601
1	California Institute of Technology 204 Karman Laboratory Main Stop 310-46 ATTN: F. E. C. Culick *1201 E. California St.* Pasadena, CA 91109
1	University of Illinois Dept. of Mechanical/Industrial Engineering ATTN: H. Krier 144 MEB; 1206 N. Green St. Urbana, IL 61801-2978
1	University of Minnesota Dept of Mechanical Engineering ATTN: E. Fletcher Minneapolis, MN 55414-3368
3	Georgia Institute of Technology School of Aerospace Engineering ATTN: B. T. Zinn E. Price W. C. Strahle Atlanta, GA 30332

No. of Copies	Organization
1	Johns Hopkins University Applied Physics Laboratory Chemical Propulsion Information Agency ATTN: T. Christian Johns Hopkins Road Laurel, MD 20707-0690
1	Massachusetts Institute of Technology Dept. of Mechanical Engineering ATTN: T. Toong 77 Massachusetts Ave Cambridge, MA 02139-4307
1	Unversity of Southern California Mechanical Engineering Dept. ATTN: OHE200, M. Gersteinutah Los Angeles, CA 90089-5199
1	University of Utah Dept. of Chemical Engineering ATTN: A. Baer Salt Lake City, UT 84112-1194
1	Washington State University Dept. of Mechanical Engineering ATTN: C. T. Crowe Pullman, WA 99163-5201
1	Rensselaer Polytechnics Institute Dept. of Mathematics Troy, NY 12181
2	Pennsylvania State University Dept. of Mechanical Engineering ATTN: K. Kuo Vogor Yang University Park, PA 16802-7501
1	California Institute of Technology Jet Propulsion Laboratory ATTN: L. D. Strand, MS 512/102 4800 Oak Grove Dr. Pasadena, CA 91109-8099
1	Stevens Institute of Technology Davidson Laboratory ATTN: R. McAlevy III Castle Point Station Hoboken, NJ 07030-5907

No. of Copies	Organization
1	Universal Propulsion Company ATTN: H. J. McSpadden 25401 North Central Ave. Phoenix, AZ 85027-7837
1	Institute of Gas Technology ATTN: D. Gidaspow 3424 S. State St. Chicago, IL 60616-3896
2	Rockwell International Rocketdyne Division ATTN: BA08, J. E. Flanagan J. Gray 6633 Canoga Ave. Canoga Park, CA 91303-2703
1	AFELM, The Rand Corporation ATTN: Library D 1700 Main St. Santa Monica, CA 90401-3297
1	General Applied Sciences Lab ATTN: J. Erdos *Merrick & Stewart Avenues* Westbury Long Island, NY 11590
2	AAI Corporation ATTN: J. Hebert J. Frankle P.O. Box 6767 Baltimore, MD 21204
1	Aerojet Solid Propulsion Corporation ATTN: P. Micheli P.O. Box 13222 Sacramento, CA 95813
1	IITRI ATTN: M. J. Klein 10 W. 35th St. Chicago, IL 60616-3799
1	Hercules, Inc. Allegheny Ballistics Laboratory ATTN: William B. Walkup P.O. Box 210 Rocket Center, WV 26726

No. of Copies	Organization
1	Hercules, Inc. Radford Army Ammunition Plant ATTN: J. Pierce Radford, VA 24141-0299
1	AVCO Everett Research Laboratory ATTN: D. Stickler 2385 Revere Beach Parkway Everett, MA 02149-5936
1	Olin Corporation Badger Army Ammunition Plant ATTN: F. E. Wolf Baraboo, WI 53913
1	Olin Ordnance ATTN: V. McDonald, Library P.O. Box 222 St. Marks, FL 32355-0222
1	Paul Gough Associates, Inc. ATTN: P. S. Gough P.O. Box 1614 1048 South St. Portsmouth, NH 03801-5423
1	Physics International Company ATTN: Library, H. Wayne Wampler 2700 Merced St. San Leandro, CA 94577-5602
2	United Technologies Corp. Chemical Systems Division ATTN: R. Brown Technical Library P.O. Box 49028 San Jose, CA 95161-9028
1	Science Applications, Inc. ATTN: R. B. Edelman 23146 Cumorah Crest Dr. Woodland Hills, CA 91364-3710
1	Thiokol Corporation Huntsville Division ATTN: Technical Library Huntsville, AL 35807

No. of Copies	Organization
1	Scientific Research Assoc., Inc. ATTN: H. McDonald P.O. Box 498 Glastonbury, CT 06033-0498
1	Veritay Technology, Inc. ATTN: E. Fisher 4845 Millersport Highway P.O. Box 305 East Amherst, NY 14051-0305
2	Thiokol Corporation Elkton Division ATTN: R. Biddle Technical Library P.O. Box 241 Elkton, MD 21921-0241
1	Battelle ATTN: TACTEC Library, J. N. Huggins 505 King Ave. Columbus, OH 43201-2693
1	SRI International Propulsion Sciences Division ATTN: Technical Library 333 Ravenswood Ave Menlo Park, CA 94025-34
	Aberdeen Proving Ground
	Cdr, CSTA
1	ATTN: STECS-PO, R. Hendricksen

INTENTIONALLY LEFT BLANK.

USER EVALUATION SHEET/CHANGE OF ADDRESS

This laboratory undertakes a continuing effort to improve the quality of the reports it publishes. Your comments/answers below will aid us in our efforts.

1. Does this report satisfy a need? (Comment on purpose, related project, or other area of interest for which the report will be used.) ________________________________

2. How, specifically, is the report being used? (Information source, design data, procedure, source of ideas, etc.) ________________________________

3. Has the information in this report led to any quantitative savings as far as man-hours or dollars saved, operating costs avoided, or efficiencies achieved, etc? If so, please elaborate. ________________________________

4. General Comments. What do you think should be changed to improve future reports? (Indicate changes to organization, technical content, format, etc.) ________________________________

BRL Report Number BRL-TR-3330 Division Symbol ____________

Check here if desire to be removed from distribution list. ____

Check here for address change. ____

Current address: Organization ____________
Address ____________

DEPARTMENT OF THE ARMY
Director
U.S. Army Ballistic Research Laboratory
ATTN: SLCBR-DD-T
Aberdeen Proving Ground, MD 21005-5066

OFFICIAL BUSINESS

BUSINESS REPLY MAIL
FIRST CLASS PERMIT No 0001, APG, MD

Postage will be paid by addressee.

NO POSTAGE NECESSARY IF MAILED IN THE UNITED STATES

Director
U.S. Army Ballistic Research Laboratory
ATTN: SLCBR-DD-T
Aberdeen Proving Ground, MD 21005-5066